

Covalently linked water-soluble fullerene–fluorescein dyads as highly efficient photosensitizers: Synthesis, photophysical properties and photochemical action



A.Yu Rybkin^{a,*}, A.Yu Belik^a, O.A. Kraevaya^{a,b}, E.A. Khakina^{a,c}, A.V. Zhilenkov^a, N.S. Goryachev^a, D. Volyniuk^d, J.V. Grazulevicius^d, P.A. Troshin^{e,a}, A.I. Kotelnikov^a

^a Institute of Problems of Chemical Physics, Russian Academy of Sciences, pr. Akademika Semenova 1, Chernogolovka, Moscow oblast, 142432, Russia

^b Higher Chemical College of Russian Academy of Sciences, D. I. Mendeleev University of Chemical Technology, Miusskaya 9, 125047, Moscow, Russia

^c A.N. Nesmeyanov Institute of Organoelement Compounds, Russian Academy of Sciences, Vavilova St. 28, Moscow, 119991, Russia

^d Department of Polymer Chemistry and Technology, Kaunas University of Technology, Radvilenu pl. 19, LT-50254, Kaunas, Lithuania

^e Skolkovo Institute of Science and Technology, Nobel st. 3, Moscow, Russia

ARTICLE INFO

Keywords:

Fullerene
Fluorescein
Dyads
Photodynamic action
Photosensitizer

ABSTRACT

The synthesis, photophysical and photodynamic properties of two water-soluble hybrid structures based on the polycationic or polyanionic fullerene [60] derivative covalently linked to fluorescein are described. The significant influence of electrostatic charges on the conformation of the studied fullerene–fluorescein structures in aqueous solution and on their photophysical properties and photochemical activity was demonstrated. A polycationic fullerene derivative–fluorescein conjugate exhibits a pronounced quenching of fluorescence (more than 25 times) due to the energy and/or electron transfer from dye to fullerene. Such activation of fullerene generates reactive oxygen species greater than 15 times more effectively than an individual dye or fullerene does. In contrast, for the polyanionic fullerene derivative–fluorescein conjugate such effects are practically absent. The demonstrated effects open up wide opportunities for a directional design of highly efficient water-soluble photosensitizers by combining the singlet-excited dyes and fullerene [60] for applications in photodynamic therapy.

1. Introduction

Photodynamic therapy is based on the effect of photoexcited molecules of dyes on biological structures. Nowadays, a rather narrow class of compounds – derivatives of porphyrin, chlorin and phthalocyanine – are used as such dyes in clinical practice [1,2]. All these types of dyes have a high quantum yield into an excited triplet state. As a result of the photoexcitation of such dyes and the further transfer of the triplet excitation or an electron from an excited dye to an oxygen molecule, reactive oxygen species (ROS) are produced, which have an enormous cytotoxic effect [1,3].

Effectiveness of a photosensitizer is determined by various factors: the quantum yield to the excited triplet state, probability of the transfer of excitation or an electron to molecular oxygen, the selectivity of accumulating the dye in a tumor and the rate of its excretion from the body, and the absorption in the red light region where biological tissues are most transparent. Improving photosensitizers for all of these parameters is relevant for photodynamic therapy.

General way of increasing triplet quantum yield of dyes is the introduction of heavy or metal atoms in their structure (Br and I, for example) [4]. However it is undesirable for photosensitizers in PDT, since it may enhance their dark toxicity *in vivo*. Designing free triplet photosensitizers without heavy atoms is highly desirable not only for photodynamic therapy but also for photocatalysis and in the triplet–triplet annihilation photon upconversion [5,6].

In the last two decades, development of new photosensitizers based on C₆₀ fullerene has been actively attempted [2,7,8]. This interest is encouraged by unique electronic, physical and biological properties of fullerenes. Fullerenes and their derivatives can selectively accumulate in biological membranes and competitively inhibit key enzyme systems [9–12]. Upon absorption of a photon, they can transform into an excited triplet state with a quantum yield close to unity [13]. Interaction of the excited fullerene with molecular oxygen with high efficiency leads to the formation of ROS. It was shown that the quantum yield of the O₂^{•−} generation by the water-soluble derivative of fullerene upon

* Corresponding author.

E-mail address: alryb@icp.ac.ru (A.Y. Rybkin).

<https://doi.org/10.1016/j.dyepig.2018.06.041>

Received 7 February 2018; Received in revised form 31 May 2018; Accepted 24 June 2018

Available online 26 June 2018

0143-7208/ © 2018 Elsevier Ltd. All rights reserved.

excitation by light (with a wavelength > 650 nm) is 77 times higher compared with the process when the commercial photosensitizer “Photosens” is used [14].

Several works were published in which the photodynamic action of fullerene and its derivatives were studied in model systems and on biological objects. A number of photodynamic and physiological effects of photoexcited fullerenes were described, including oxidative damage of membrane lipids [15], induction of cytotoxic effects *in vitro* [16–18] and *in vivo* [19,20], and also inactivation of bacteria [21–23] and viruses [24,25].

Despite the pronounced photodynamic effect of native fullerenes and their derivatives, the possibility of their wide application in clinical practice is significantly limited by their low water solubility and weak absorption in the visible (especially the red) region of the spectrum. This problem could be solved by constructing one molecular structure combining a fullerene derivative having a high solubility in water and a dye that will effectively absorb light in the visible region of the spectrum and transfer excitation energy or an electron to fullerene C₆₀.

In our previous works, we demonstrated the possibility to significantly enhance the photodynamic activity of the water-soluble polycationic fullerene derivative (PCFD) by forming non-covalent complexes with various dyes: fluorescein [26], eosin [27], erythrosine [28] and a commercial photosensitizer “Photosens” (phthalocyanine derivative) [14]. Upon photoexcitation of the complex PCFD-“Photosens” in the absorption band of the dye ($\lambda > 650$ nm), its photodynamic activity increased by 20 times compared with the activity of the individual “Photosens” and 108 times compared with PCFD [14]. Moreover, it was shown for all studied dyes that the enhancement of the photodynamic activity of the complex occurs due to the excitation of the dye into the excited singlet state and further transfer of the excitation or an electron to the fullerene core.

The same effect of energy transfer from the singlet excited state of the dye to the fullerene core was previously demonstrated for non-covalent fullerene–dye complexes [29,30] and for covalent fullerene–dye dyads [31–34] in organic solvents. Nevertheless, such structures are not suitable for applications in photodynamic therapy because of their low solubility in water.

Although the water-soluble non-covalent fullerene–dye complexes demonstrated pronounced photodynamic activity in aqueous solutions [14,26–28], further studies did not show the same effect on cell cultures *in vitro*. It is known that water-soluble fullerene derivatives have pronounced amphiphilic properties and can be incorporated into the lipid bilayer of model biological membranes [9,35]. This can lead to the destruction of non-covalent fullerene–dye complexes when they interact with cell membranes.

To create new effective fullerene–dye photosensitizers, it is necessary to develop methods for synthesizing water-soluble structures that would be stable in heterogeneous biological media – protein solutions and lipid membranes. We previously synthesized two water-soluble dyads by covalently attaching polyanionic fullerene derivatives to ruboxyl, a derivative of doxorubicin, an anthracycline antibiotic [36]. These fullerene–ruboxyl dyads showed a significant enhancement of the photodynamic action compared with the individual fullerene derivative in aqueous solution upon excitation in the absorption band of ruboxyl. At the same time, ruboxyl itself did not exhibit any photodynamic activity.

Several articles on covalent fullerene–doxorubicin dyads with photoinduced antitumor activity have been published [37,38]. We note that ruboxyl, as well as doxorubicin, does not have a significant quantum yield to the excited triplet state. As was described for non-covalent fullerene–dye complexes, the photodynamic action of these covalent dyads is increased because of the transfer of the excitation and/or an electron from the singlet excited state of the dye to the fullerene core followed by generation of ROS. A similar effect of fullerene photoactivation was observed for covalent fullerene–dye dyads with rhodamine, chlorin and other dyes [39–41].

In this paper, we report the synthesis of two water-soluble covalently-linked dyads based on polycationic or polyanionic fullerene derivative and a fluorescein dye and the results of a comparative study of the photophysical properties and photodynamic activity of these dyads in aqueous solutions.

2. Experimental

2.1. Reagents

NADH (Nicotinamide adenine dinucleotide, Sigma), NBT (nitro blue tetrazolium chloride, Sigma), fluorescein sodium salt (Sigma), FITC (fluorescein-5-isothiocyanate, Serva) and EDTA (ethylenediaminetetraacetic acid, Sigma) were used.

2.2. Synthesis of water-soluble fullerene–fluorescein dyads PCFD-FI and PAFD-FI

Polycationic and polyanionic fullerene derivatives (PCFD and PAFD) were synthesized according to the previously reported procedures and characterized (PCFD is a compound **1f** in Ref. [42] and PAFD – compound **2a** in Ref. [43]). The covalent conjugate of PCFD with fluorescein (PCFD-FI) was synthesized according to Scheme 1 using the following procedure.

PCFD-FI: The fullerene derivative PCFD (100 mg, 0.06 mmol, 1.0 eq.) was dissolved in 6 mL of methanol under gentle magnetic stirring at room temperature. The solution of FITC (28 mg, 0.07 mmol, 1.2 eq.) and triethylamine (7.2 mg, 0.07 mmol, 1.2 eq.) in methanol (6 mL) was added to PCFD in one portion. The reaction mixture was stirred at room temperature for 2 days. The solvent was then removed in vacuum, and the residue was washed with diethyl ether and dried in air. PCFD-FI was obtained as a light-brown powder with a quantitative yield.

¹H NMR (500 MHz, MeOD): $\delta = 6.76$ – 6.69 (m, 4H), 6.67 – 6.62 (m, 2H), 6.59 – 6.55 (m, 3H), 4.11 (br.s, 2H, NH), 3.77 – 3.53 (m, 10H, CH₂), 3.46 – 3.39 (m, 10H, CH₂) ppm. UV/VIS (DMSO, $\epsilon/M^{-1}cm^{-1}$): $\lambda = 307$ (30.6×10^3), 330 (29.5×10^3), 363 (23.5×10^3), 417 (9.4×10^3), 483 (3.7×10^3) nm.

FT-IR (KBr pellet): $\nu = 522$ (W), 542 (W), 578 (W), 598 (W), 674 (W), 722 (M), 766 (W), 798 (M), 838 (M), 902 (W), 958 (W), 994 (W), 1038 (W), 1082 (M), 1134 (S), 1182 (S), 1204 (VS), 1258 (M), 1324 (M), 1386 (M), 1438 (M), 1458 (M), 1506 (M), 1540 (M), 1610 (M), 1634 (S), 1676 (VS), 2854 (M), 2924 (M), 3046 (M) cm^{-1} .

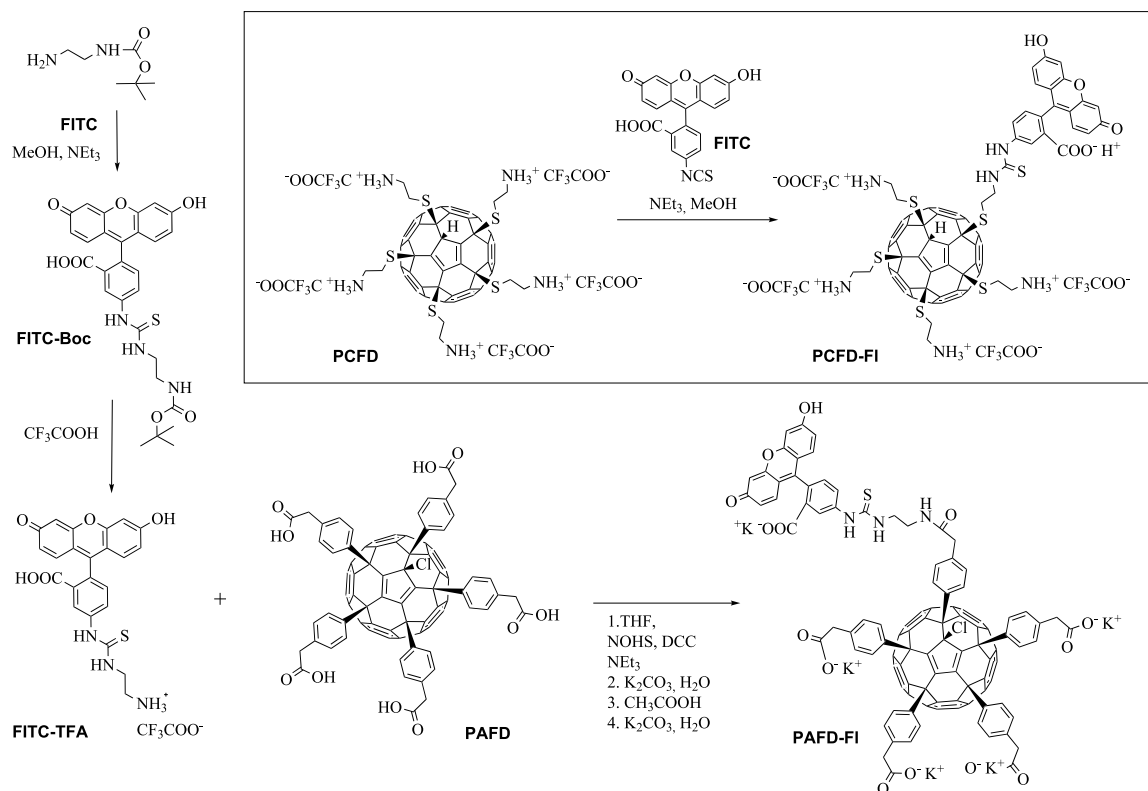
The conjugate PAFD-FI was synthesized in three steps according to Scheme 1.

FITC-Boc: *tert*-butyl (2-aminoethyl)carbamate (49.4 mg, 0.3082 mmol) and distilled methanol (3 mL) were placed under argon in a two-necked flask. The solution of FITC (100 mg, 0.2568 mmol) in distilled methanol (6 mL) and 50 mL of triethylamine was added dropwise to the reaction mixture. The obtained reaction mixture was stirred vigorously for 72 h. The solvent was removed in a rotary evaporator, the residue was washed with diethyl ether (20 mL) and dried. The obtained FITC-Boc (134 mg, 95%) was stored in the freezer.

¹H NMR (500 MHz, MeOD): $\delta = 8.17$ (s, 1H), 7.98 (s, 1H), 7.90 (d, 1H), 7.74 (d, 1H), 7.24 – 7.32 (m, 1H), 7.19 (d, 2H), 6.96 (s, 1H), 6.65 (m, 5H), 3.28 (t, 2H, CH₂), 2.95 (t, 2H, CH₂), 1.48 (s, 9H, CH₃) ppm.

FITC-TFA: FITC-Boc (134 mg, 0.244 mmol) and trifluoroacetic acid (TFA, 5 mL) were placed in a 50 mL round bottom flask, and the reaction mixture was stirred for 15 min at room temperature. The excess TFA was then removed in a rotary evaporator, and the residue was washed with diethyl ether (3×20 mL) and dried in air. The yield of the obtained FITC-TFA was 86% (118 mg).

PAFD-FI: The fullerene derivative PAFD (50 mg, 0.0349 mmol), *N*-hydroxysuccinimide (4.5 mg, 0.0384 mmol) and freshly distilled THF (3 mL) were placed under argon in a two-necked flask. The reaction mixture was stirred for 10 min, and the solution of dicyclohexylcarbodiimide (7.9 mg, 0.0384 mmol) in THF (2 mL) was then added.



Scheme 1. Synthesis of the conjugates **PCFD-FI** and **PAFD-FI**.

The obtained reaction mixture was stirred vigorously for 12 h. The solution of FITC-TFA (21 mg, 0.0384 mmol) and 50 mL of triethylamine in distilled water (1.5 mL) was added dropwise, and the reaction mixture was stirred for another 12 h. K₂CO₃ (12 mg, 0.0873 mmol) in distilled water (3 mL) was then added to the reaction mixture, and THF was removed in a rotary evaporator. The obtained aqueous solution was filtered through a 0.45 μm PES syringe filter and quenched with acetic acid (1 mL). The obtained precipitate was centrifuged, washed with distilled water and dried in vacuum. The conjugate **PAFD-FI** (acid form) was obtained as a brown powder with a yield of 32 mg (49%).

ESI MS: $m/z = 1862$ ($[M-H]^+$).

¹H NMR (500 MHz, CS₂: acetone-*d*₆: DMSO-*d*₆): δ = 8.70–6.90 (m, 29H), 4.20–3.90 (m, 14H), 8.49–8.41 (m, 1H), 8.37 (d, 1H), 8.35–8.22 (m, 3H), 8.20 (d, 1H), 8.16–8.13 (m, 1H), 8.12–8.11 (m, 1H), 8.10–8.07 (m, 2H), 7.87–7.73 (m, 9H), 7.71–7.67 (m, 2H), 7.63 (d, 2H), 7.60–7.58 (m, 1H), 7.57–7.42 (m, 2H), 7.15–7.11 (m, 2H), 7.09–7.06 (m, 1H), 7.04 (br.s, 1H), 7.02–6.99 (m, 1H), 4.08–4.07 (m, 4H, CH₂), 4.04 (s, 2H, CH₂), 4.02–3.99 (m, 2H, CH₂), 3.93–3.92 (m, 2H, CH₂), 3.89–3.85 (m, 4H, CH₂) ppm.

FT-IR (KBr pellet): ν = 542(W), 1114(W), 1178(M), 1236(M), 1258(M), 1286(M), 1312(W), 1386(M), 1418(M), 1438(W), 1450(W), 1460(M), 1510(M), 1534(W), 1542(M), 1560(M), 1610(M), 1618(M), 1636(M), 1708(M), 2924(W), 3008(W), 3028(W), 3038(W), 3074(W), 3096(W), 3112(W), 3426(VS), 3432(VS), 3442(VS), 3588(M), 3630(W) cm⁻¹.

PAFD-FI (acetic form) (32 mg, 0.017 mmol) was suspended in 5 mL of distilled water, and anhydrous K₂CO₃ (5.9 mg, 0.043 mmol) was added. The obtained aqueous solution was filtered through a PES syringe filter and freeze-dried yielding 31 mg (90%) of **PAFD-FI** (potassium salt).

2.3. Computational simulation of PAFD-FI and PCFD-FI structures

The dyads **PAFD-FI** and **PCFD-FI** were geometrically optimized with a semi-empirical quantum chemistry method using the MOPAC2016

package [44] with PM7 and COSMO parameterization methods to account for the surrounding water [45].

2.4. Dynamic light-scattering experiments

Aqueous solutions of fullerene derivatives (10⁻⁵ M) were filtered through 0.45 μm PES syringe filters and poured into vials that were prewashed several times with filtered water to remove dust particles. The solutions were then thermostated for about 15 min at 20 °C thus allowing the systems to reach equilibrium. The temperature control accuracy was 0.1 °C. Dynamic light-scattering (DLS) measurements were performed at a detection angle of 90° with a Photocor Complex (Photocor Instruments Inc., USA; <http://www.photocor.com>) setup equipped with a TEC stabilized diode laser (λ = 790 nm). The mutual diffusion coefficients of fullerene aggregates were computed from the DLS data using the DynaLS program (Alango, Israel). Hydrodynamic diameters of the fullerene aggregates were calculated from the mutual diffusion coefficients using the Einstein–Stokes formula for diffusion coefficients of spherical particles. The viscosity (η = 1.006) and the refractive index (n = 1.33268) of water were used.

2.5. Photophysical and photochemical studies

Absorption spectra were measured using a Cary-60 spectrophotometer equipped with a thermostated cell. Fluorescence steady-state spectra and fluorescence quantum yield of the dyes under study were recorded by an FLS980 spectrometer (Edinburgh Instruments) and by a Cary-Eclipse fluorescence spectrophotometer. The fluorescence decay kinetics were measured with a 16-channel PML-Spec detector using a time-correlated SPC-530 photon counter (Becker & Hickl GmbH) with a time resolution of 2.4 ps. A sample was excited by a picosecond LDH-P-C-470 laser (PicoQuant GmbH) (λ = 470 nm, τ_{1/2} ≤ 300 ps, E = 1 mW). The fluorescence lifetime was calculated by exponential approximation at the maximum of the emission spectrum. The photodynamic properties of the studied compounds were

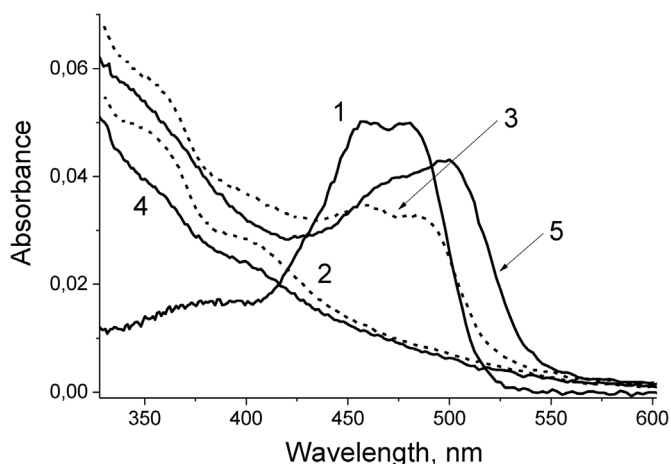


Fig. 1. Absorption spectra of fluorescein (1), PAFD (2), covalent dyad PAFD-FI (3), PCFD (4) and covalent dyad PCFD-FI (5) at a concentration of $2 \cdot 10^{-6}$ M in water (pH = 6.5).

investigated using the illumination provided by a high-pressure xenon lamp (150 W) passed through a system of optical filters selecting the 450–550 nm band (which corresponds to the absorption maximum of fluorescein). The power of the light illuminating the sample was $\sim 4.4 \text{ mW cm}^{-2}$. Photochemical reactions were performed in a $1 \times 1 \text{ cm}$ quartz cuvette illuminated inside a temperature-controlled sample unit stabilized at 20°C . The cuvette was filled with 2 mL bi-distilled water, (pH = 6.5) containing NADH ($4 \cdot 10^{-4} \text{ M}$), NBT ($4.8 \cdot 10^{-5} \text{ M}$), EDTA ($2 \cdot 10^{-5} \text{ M}$) and the studied compounds (Scheme 1) were then added to achieve a concentration of $2 \cdot 10^{-6} \text{ M}$. The photochemical activity of the compounds (relative amount of superoxide radicals produced) was investigated using a standard formazan assay by measuring the evolution of the optical density at 560 nm [46].

The formula

$$E_c = \frac{D_{\text{dyad}} - D_{\text{control}}}{(D_{\text{PFD}} - D_{\text{control}}) + (D_{\text{dye}} - D_{\text{control}})} \quad (1)$$

was used to calculate the enhancement coefficient E_c of relative photodynamic activity for dye–PFD dyads in water, where the values D is an optical density change at 560 nm for the indicated compounds after 5 min of photoirradiation.

3. Results and discussion

3.1. Approach justification

The choice of fluorescein as a photosensitizer used for conjugation with the two types of fullerene derivatives, cationic and anionic, was motivated by the following reasons. As described in papers [26–28], fluorescein, as well as other xanthene dyes eosin and erythrosine, acts as a highly active photosensitizer in the presence of the water-soluble polycationic fullerene derivative. It was demonstrated that the negatively charged fluorescein in aqueous solutions forms stable complexes by reaction with the oppositely charged cationic fullerene derivative. In such a hybrid structure, the electron or energy transfer can occur from the singlet excited state of the dye to the fullerene core followed by the generation of ROS. The efficiency of the generation of ROS in the structure of these complexes increased in the sequence erythrosine < eosin < fluorescein, depending on the quantum yield of dyes to the singlet excited state [28]. But these complexes did not have an increase of photodynamic effect in cells *in vitro*, which can be explained by the disintegration of the non-covalent complexes as a result of the fullerene derivatives interacting with biological membranes. We can conclude that for biomedical applications, it is necessary to design stable

covalently linked fullerene–dye dyads.

Covalently linked fullerene–fluorescein dyads were previously reported only as fluorescent probes for cellular uptake study of fullerene derivatives [47–49] without evaluation of their photodynamic activity.

It is known that the photodynamic action of compounds, including fullerene derivatives, depends greatly on the electrostatic charges of molecules [40,50,51]. Our goal here is to create photoactive compounds – stable dyads based on the dye fluorescein (with two negative charges) covalently linked to water-soluble fullerene derivatives with five various charges (negative or positive).

The fullerene derivatives PAFD and PCFD have a superior molecular structure: all five organic addends bearing solubilizing carboxylic or amino groups are attached to one hemisphere of the fullerene molecule around a central pentagon unit thus leaving the rest of the carbon cage available for interactions (especially hydrophobic) with different biological targets. We have previously shown that such molecular structures demonstrate expressed membranotropic properties [35] and different types of pronounced neuroprotective [52] and antiviral activity in combination with a low toxicity [43,53]. Another advantage of PAFD or PCFD compounds is their exceptionally high ($> 100 \text{ mg mL}^{-1}$) solubility in water in the form of sodium or potassium salts, which allows an easy administration to biological systems varying from cell cultures to living animals. One or more carboxylic or amino groups in the PAFD or PCFD molecules can be potentially coupled with the fluorescein-5-isothiocyanate (FITC) units using a standard carbodiimide approach or direct attachment (see Experimental). Our previous experience showed that it is necessary to keep at least four ionogenic groups to maintain the solubility of the fullerene derivative in water on a reasonable level of $1\text{--}10 \text{ mg mL}^{-1}$. Here we intentionally performed the coupling of the fullerene derivatives PAFD and PCFD with just one FITC molecule per fullerene cage.

3.2. Photophysical properties of conjugates PAFD-FI and PCFD-FI

The absorption spectra of the conjugates PAFD-FI and PCFD-FI in a first approximation were shown to be a superposition of the absorption spectra of fluorescein and the fullerene derivative PAFD or PCFD (Fig. 1), but fluorescein moiety shows remarkable variations in intensity and position of absorption spectra. As shown in Fig. 1, spectra of fluorescein in the conjugates decreased in intensity for both conjugates and moved to the red region by about 20 nm for the compound PCFD-FI (FITC conjugate with cationic fullerene derivative). We can assume that the interaction of the negatively charged fluorescein moiety with the fullerene spheroid is more intense in the case of this cationic derivative.

The fluorescence spectra of PAFD-FI and PCFD-FI are positioned similarly to the fluorescence of fluorescein with a band maximum 515 nm (in comparison with band maximum 513 nm for fluorescein) (Fig. 2).

A study of the luminescent properties of the covalently linked dyad PCFD-FI showed that the fluorescence of the dye in its structure was significantly quenched 25.9 times compared with the fluorescence of the free dye (taking the variation of dye's extinction at $\lambda_{\text{ex}} = 490 \text{ nm}$ into account; Fig. 2). This is in excellent agreement with the literature data – strong fluorescence quenching was reported for the majority of fullerene–dye structures [34,54,55], including all fullerene–fluorescein dyads in aqueous solution [47–49]. This indicates an effective transfer of the excitation or an electron from a dye excited in the singlet state to the fullerene core in the dyad. On the other hand, the dyad PAFD-FI has strong fluorescence: it is only 10% weaker than the fluorescence of the free fluorescein (Fig. 2).

The fluorescence decay kinetics of the dyads under study showed that the fluorescence decay time of the PAFD-FI (with the anionic derivative of fullerene PAFD) is $3.82 \pm 0.02 \text{ ns}$ and practically does not differ from the decay time of free fluorescein ($3.85 \pm 0.03 \text{ ns}$; Fig. 3 and Table 1, line 4), although it has slightly lower fluorescence intensity. The fluorescence lifetime of the PCFD-FI dyad (with the

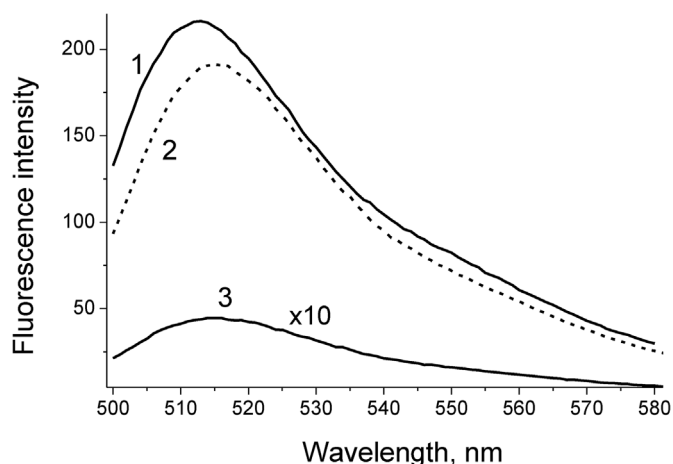


Fig. 2. Fluorescence spectra of fluorescein (1), covalent dyad PAFD-FI (2) and covalent dyad PCFD-FI (3, fluorescence intensity is multiplied by a factor of 10) at a concentration of $2 \cdot 10^{-6}$ M in water (pH = 6.5). $\lambda_{\text{ex}} = 490$ nm, $\lambda_{\text{em}} = 515$ nm.

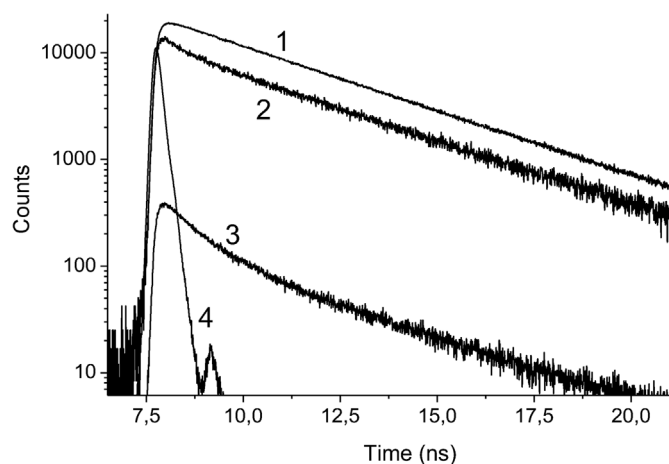


Fig. 3. Fluorescence decay profiles of fluorescein (1), covalent dyad PAFD-FI (2) and covalent dyad PCFD-FI (3) at a concentration of $2 \cdot 10^{-6}$ M in water (pH = 6.5). $\lambda_{\text{ex}} = 470$ nm, $\lambda_{\text{em}} = 515$ nm. The instrument response function is also shown (4).

Table 1

A comparison of photophysical properties and photochemical activity of the covalent dyads PAFD-FI and PCFD-FI.

	Fluorescein	dyad PAFD-FI	dyad PCFD-FI
1 Solubility in water, mg/ml	> 50	≤ 40	$\leq 2^a$
2 Absorbance λ_{max} , nm	480	484	500
3 Fluorescence λ_{max} , nm	513	515	516
4 Fluorescence lifetime of covalent dyad in water, ns	3.85 ± 0.03	$\tau_1 = 0.60 \pm 0.05$ $\tau_2 = 3.82 \pm 0.02$	$\tau_1 = 0.79 \pm 0.04$ $\tau_2 = 3.94 \pm 0.02$
5 Fractional intensities of the positive fluorescence decay components ($A \cdot \tau$), %	–	$A_1 \cdot \tau_1 = 5.9$ $A_2 \cdot \tau_2 = 94.1$	$A_1 \cdot \tau_1 = 8.3$ $A_2 \cdot \tau_2 = 91.7$
6 Length of linker between fluorescein and fullerene core, Å	–	17.4	10.8
7 The straight line distance between fluorescein and fullerene core, Å	–	13.9	7.2
8 The Förster distance R_0 , Å	–	39	–
9 Maximum of photoinduced electron transfer (ET) distance, Å	–	8^b	–
10 Degree of fluorescence quenching I_0/I (experimental), fold	–	1.1	25.9
11 Fluorescence quenching I_0/I (calculated by FRET theory), fold	–	44	1450
12 Fluorescence quenching I_0/I (calculated by ET theory with $R =$ straight line distance, $\alpha = 1.4 \text{ Å}^{-1}$), fold	–	~ 1	2.6
13 Fluorescence quenching I_0/I (calculated by ET theory with $R =$ length of linker, $\alpha = 0.9 \text{ Å}^{-1}$), fold	–	~ 1	5.0
14 DLS average hydrodynamic sizes (R_h), nm	–	527 ± 62	621 ± 153
15 Enhancement coefficient (E_c) of photochemical activity of covalent dyad fluorescein-PFD in water	–	1.24	15.15

^a Powder of covalent dyad PCFD-FI is readily solubilized in pure ethanol or DMSO. Obtained solution of the dyad ($5 \cdot 10^{-3}$ M) was diluted to required concentration with water.

^b For excited singlet states with $3.9 \cdot 10^{-9}$ s lifetime, in accordance with Eq. (4).

cationic fullerene derivative) is 0.09 ns longer than the fluorescence lifetime of free fluorescein, (3.94 ± 0.02 ns; Table 1, line 4 and Fig. 3), and its fluorescence intensity is significantly lower compared with the free dye and the PAFD-FI dyad.

At the same time, all dyads under study have a noticeable contribution of the fast component τ_1 with fluorescence lifetimes of 0.60–0.79 ns (Fig. 3 and Table 1, line 4). Its relative intensity varies from 5.9% to 8.2% of the total fluorescence signal for PAFD-FI and PCFD-FI (Table 1, line 5).

Considering all given data, we can assume that the significant shift in the absorption spectrum of the fluorescein fragment in the dyad PCFD-FI and strong fluorescence quenching is a result of the effective interaction of a fluorescein moiety with fullerene core. This interaction is much less pronounced in the case of the dyad PAFD-FI.

3.3. Computational modeling of PCFD-FI and PAFD-FI spatial structures

Differences in the observed effects for PCFD-FI and PAFD-FI can be explained by electrostatic interactions between the dye and the fullerene moiety both within the molecular structures of the dyads and between molecules.

As mentioned above, the excitation of the dye to the excited singlet state in such a fullerene–dye structure can lead to energy or electron transfer to the fullerene core. It is known that the transfer efficiency of energy or an electron strongly depends on the distance R separating the donor and the acceptor: as $1/R^6$ for the Förster resonance energy transfer (FRET) mechanism [56] and exponentially as $\exp(-\alpha R)$ for electron transfer (ET) [57–59].

As can be calculated from the structural formula of the dyads under study, the length of the linker between the fluorescein and the fullerene core in the PCFD-FI (10.8 Å) is significantly shorter than in the PAFD-FI (17.4 Å), as shown in Fig. 5 and Table 1, line 6. In addition, the presence of charges on the dye and on the fullerene adds in the dyads can significantly affect their conformation and consequently the distance between the dye moiety and fullerene core.

The PCFD-FI and PAFD-FI spatial structures were modeled computationally by geometrically optimizing them with a semi-empirical quantum chemistry method using the MOPAC2016 package with PM7 and COSMO parameterization methods to account for the surrounding water (see Experimental). As a result of the calculations, it was found that the molecular structure of the PCFD-FI is most likely in the folded state as a result of the electrostatic interaction of the negatively charged carboxyl group of fluorescein and the positively charged amino group

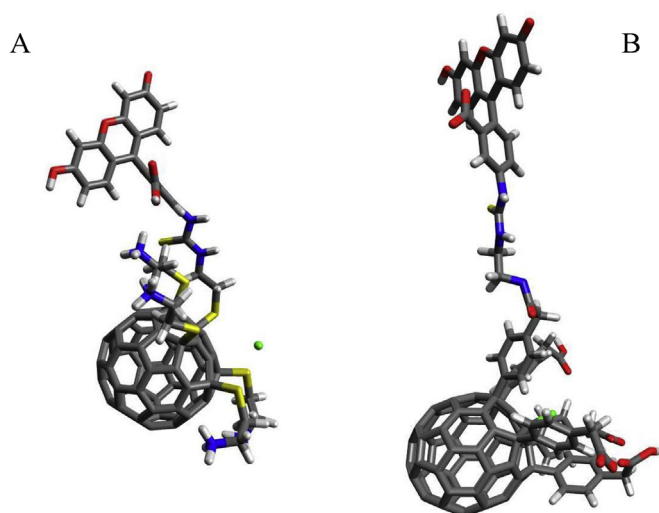


Fig. 4. Calculated conformation of PCFD-FI (A) and PAFD-FI (B). using MOPAC2016 with the PM7 and COSMO methods.

on one of PCFD addends. As a result, the fluorescein moiety is approximated to the surface of the fullerene core by a distance of 7.2 Å (Fig. 4, A, and Table 1, line 7). In contrast, the structure of PAFD-FI is most likely to be in the unfolded state as a result of the electrostatic repulsion of the same negative charges on the dye and on fullerene addends. As a result, the distance between dye moiety and the fullerene core in PAFD-FI is increased up to 13.9 Å (Fig. 4, B and Table 1, line 7).

The electrostatic interaction between the negatively charged fluorescein moiety and the positively charged fullerene addends in the PCFD-FI thus facilitates their approach, which increases quenching of the excited singlet state of fluorescein by the mechanism of electron

and/or energy transfer to the fullerene core. In contrast, it can be assumed that for the PAFD-FI, the fullerene and the dye are spaced as far apart as possible as a result of the electrostatic repulsion of the negative charges on the fullerene and dye moiety. The excitation or electron transfer in the latter dyad is therefore significantly obstructed.

3.4. Fluorescence quenching analysis in PCFD-FI and PAFD-FI by Förster and electron transfer theories

Based on the structural data, it is possible to calculate the degree of fluorescence quenching of the dye in the dyads under study.

3.4.1. Fluorescence quenching by energy transfer

According to the FRET theory [56], the distance R_0 at which the fluorescence quenching by 50% should occur can be calculated by the formula

$$R_0^6 = 8.79 \times 10^{-5} (\kappa^2 n^{-4} Q_D J(\lambda)) (R_0 \text{ in } [\text{Å}], \text{ if } \lambda \text{ in } [\text{nm}]) \quad (2)$$

where Q_D is the quantum yield of the donor fluorescence in the absence of the acceptor, $J(\lambda)$ is the overlap integral, n is the refractive index of the solvent and k is the orientation coefficient depending on the directions of the dipole moments of the transition. In systems with disordered orientations of the dipole moments of the transition, it is usually assumed that $k^2 = 2/3$.

With the value of R_0 and the calculated distance R between donor and acceptor units, the efficiency (the ratio I_0/I) of fluorescence quenching due to the excitation transfer can be estimated by the formula

$$\frac{I_0}{I} = \left(\frac{R_0}{R} \right)^6 + 1 \quad (3)$$

where I_0 is the fluorescence intensity in the absence of the acceptor and I is the fluorescence intensity in the presence of the acceptor.

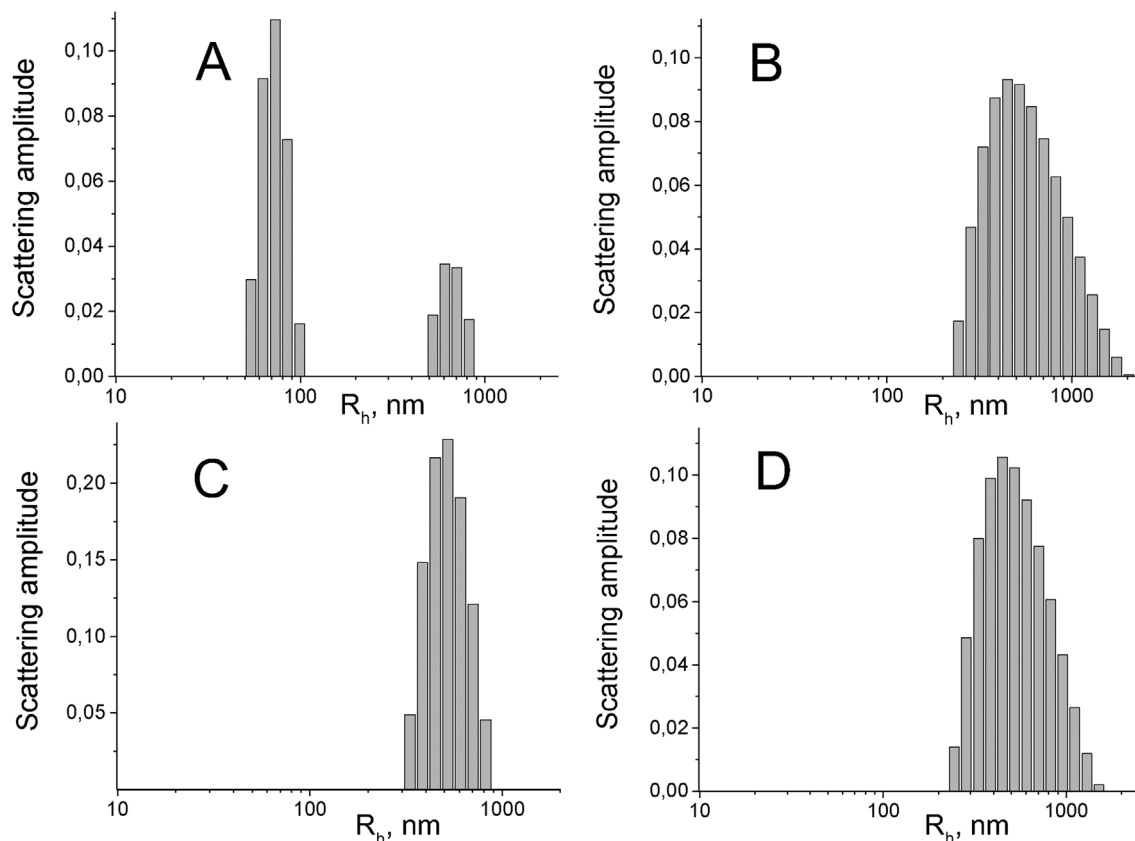


Fig. 5. DLS profiles of aqueous solutions of fullerene derivatives (10^{-5} M): A – PCFD; B – PCFD-FI; C – PAFD; D – PAFD-FI.

Therefore, under the assumption that the energy transfer occurs between interacting dipoles placed at the center of conjugate structure of the dye and at the center of the fullerene core (the distances are 11.55 Å for **PCFD-FI** and 20.85 Å for **PAFD-FI**), the fluorescence of the **PCFD-FI** can be quenched up to 1450 times compared with the free dye and up to 44 times for in the **PAFD-FI**. But the obtained quenching estimates are 40–55 times higher than the experimental fluorescence quenching data (quenching 25.9 times for **PCFD-FI** and 1.1 times for **PAFD-FI**, as shown in Table 1, lines 10 and 11). This discrepancy can be explained by the fact that the orientation factor k^2 was taken equal to 2/3 in the calculation, as for randomly arranged molecules. In the case of the studied dyads, the mutual orientation of the dipole moments of optical transitions in fluorescein and fullerene could be substantially limited, which could significantly affect the value of the orientation factor, reducing it to less than 0.02.

3.4.2. Fluorescence quenching by electron transfer

In the case of the theoretical electron transfer mechanism [60,61], under optimal conditions (when the absolute values of the free energy ΔG of the reaction and the energy λ of the nuclear energy reorganization are equal), the constant k_{et} can be estimated by the empirical formula

$$k_{et} = k_0 \exp(-\alpha R) \quad (4)$$

which was obtained as a result of generalizing the electron transfer data in various molecular structures including photoexcited molecules [57–59]. Here, $k_0 = 10^{13} \text{ s}^{-1}$, R is the distance between the donor and acceptor (between the π -orbitals of the dye and fullerene core for **PCFD-FI** and **PAFD-FI**), α is the parameter characterizing the influence of the environment on the overlap of the donor and acceptor wave functions due to the superexchange interaction.

Depending on the type of matrix separating the donor and acceptor (e.g., a saturated hydrocarbon chain, a polypeptide chain, packed differently, in water or vacuum), the value α can differ: 0.9 \AA^{-1} for saturated hydrocarbon chains, 1.4 \AA^{-1} for transport in a protein globule structure by the shortest distance between donor and acceptor, $1.8\text{--}2.4 \text{ \AA}^{-1}$ for water molecules [57–59].

In the case of the **PCFD-FI** and **PAFD-FI** dyads, two transport paths can be considered (Scheme 1, Fig. 5 and Table 1, line 6 and 7):

1. the shortest path between the π -orbitals of the dye and fullerene core;
2. along the linker chain between fluorescein and fullerene.

In the first case, the shortest distance is 7.2 Å for **PCFD-FI** and 13.9 Å for **PAFD-FI**. The linker chain length is 10.8 Å for **PCFD-FI** and 17.4 Å for **PAFD-FI**.

Using Eq. (4), we can estimate that k_{et} in the **PCFD-FI** case should be $0.42 \times 10^9 \text{ s}^{-1}$ for electron transfer by the shortest distance ($\alpha = 1.4 \text{ \AA}^{-1}$) and $0.6 \times 10^9 \text{ s}^{-1}$ for transport along a linker chain ($\alpha = 0.9 \text{ \AA}^{-1}$). As a result, with the free fluorescein lifetime of $3.85 \times 10^{-9} \text{ s}$ taken into account, the fluorescence of the dye in the **PCFD-FI** should be quenched 2.6–5 times compared with free fluorescein (Table 1, lines 10, 12 and 13). At the same time, the experimentally observed quenching of fluorescence for a given dyad is more than 5–10 times higher (Table 1, line 10). This discrepancy can be explained by a contribution of the FRET quenching mechanism, which was discussed above.

Unlike **PCFD-FI**, the fluorescence of **PAFD-FI** should not be quenched at all, because it was estimated by the electron transfer mechanism using Eq. (4) and the parameters $\alpha = 1.4 \text{ \AA}^{-1}$ at $R = 13.9 \text{ \AA}$ or $\alpha = 0.9 \text{ \AA}^{-1}$ at 17.4 \AA (Table 1, lines 12 and 13). This result agrees well with the experimental data (quenching 1.1 times, Table 1, line 10). Photoinduced electron transfer for **PAFD-FI** is significantly obstructed because of the large distance between the dye and the fullerene core.

3.5. Formation of supramolecular nanostructures by **PCFD-FI** and **PAFD-FI**

We note that quenching of the singlet excited state of fluorescein is possible not only by excitation or electron transfer between the dye and fullerene within a single dyad molecule but also by intermolecular interactions between the dye of one dyad with the fullerene core of another dyad molecule. Obviously, such interactions due to diffusion of individual dyads are impossible in our case because the experiments were performed at dyad concentrations of $2 \cdot 10^{-6} \text{ M}$ and the collision frequency of molecules in an aqueous solution at such concentrations is lower than $1/\tau_{(FL)} = 0.26 \cdot 10^9 \text{ s}^{-1}$ by several orders of magnitude.

At the same time, the fact of the formation of stable complexes between cationic fullerene derivative and negatively charged xanthenes dyes fluorescein, eosin and erythrosine, as well as the phthalocyanine dye “Photosens,” was experimentally demonstrated in aqueous solutions [14,27,28]. The formation of complexes between hydrophobic dyes and fullerenes in organic solvents has also been described [55,62]. Amphiphilic fullerene derivatives can also form nanostructures (“nanosomes”) like liposomes from natural or synthetic lipids [63,64].

Based on the above facts, we can assume that the amphiphilic derivatives of fullerenes **PCFD** and **PAFD**, as well as **PCFD-FI** and **PAFD-FI** dyads, can interact with one another in aqueous solutions forming stable nanostructures. To verify this assumption, we studied the aqueous solutions of fullerene derivatives **PCFD** and **PAFD**, as well as **PCFD-FI** and **PAFD-FI** dyads, by the DLS method. It was found that all compounds under study formed well-organized supramolecular architectures with average hydrodynamic sizes ranging from 75 to 620 nm (Fig. 5 and Table 1, line 14). As previously shown by the pulsed field gradient NMR method, this type of fullerene derivatives tend to form associates whose size depends on the type of solvent; the strongest aggregation was observed for aqueous solutions [65]. Moreover, as shown by the DLS method, similar fullerene–ruboxyl dyads have an average hydrodynamic radius of 85–100 nm [36].

The size of the associates of the polycationic **PCFD-FI** dyad is markedly increased compared with the original **PCFD** (Fig. 5A and B). In contrast, the polyanionic **PAFD-FI** dyad has no significant change in the size of associates compared with the original fullerene derivative **PAFD** (Fig. 5C and D). The observed effect in the first case may indicate the interaction of positively charged fullerene derivative addends of one dyad molecule with negatively charged fluorescein moiety of neighboring dyads, leading to an increase in the size of the associates and a significant fluorescence quenching in aqueous solutions.

In such nanostructures, the fluorescein moieties and fullerene core of various dyads can interact with each other by both static and dynamic mechanisms, which also lead to fluorescence quenching of the dye. These interactions can lead both to transfer of excitation from the fluorescein fragment to the fullerene nucleus and to stimulation of the intercombination conversion of fluorescein into a triplet state. In the latter case, the fullerene core can act as a heavy atom, shortening the lifetime of the excited singlet state of the fluorescein fragment from 3.8 ns to 0.8 ns, as was observed for the fluorescein derivative with two iodine atoms in its structure [66]. This assumption is supported by the fact that for all the studied dyads, a fast fluorescence component with lifetimes 0.60–0.79 ns was observed (Fig. 3 and Table 1, line 4).

3.6. Photodynamic activity of **PAFD-FI** and **PCFD-FI** in aqueous solution

To clarify the effect of ROS generation in aqueous solutions by water-soluble fullerene–fluorescein structures, we investigated the comparative efficacy of $\text{O}_2^{\cdot -}$ superoxide radical generation by the compounds **PAFD-FI** and **PCFD-FI**.

As can be seen from Fig. 6, after photoexcitation in the 450–550 nm region, the compounds **PAFD-FI** and **PCFD-FI** and also the reference samples (fluorescein, **PAFD**, and **PCFD**) have different photodynamic activities. It can be estimated that the photodynamic activity of the cationic compound **PCFD-FI** exceeds the respective similar activities of

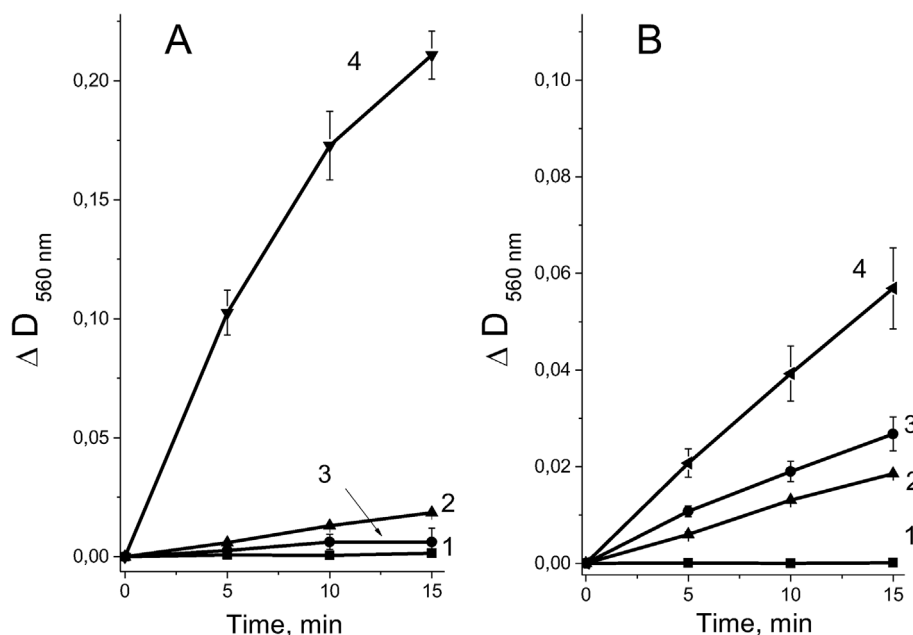


Fig. 6. Kinetics of $O_2^{\cdot -}$ formation as a result of the photochemical reaction in water under visible light irradiation in the wavelength range of 450–550 nm sensitized by different compounds: A: control (1), fluorescein (2), PCFD (3), covalent dyad PCFD-FI (4). B: control (1), fluorescein (2), PAFD (3), covalent dyad PAFD-FI (4).

the anionic compound PAFD-FI, fluorescein and the fullerene derivatives PAFD and PCFD about 3.7, 11, 8 and 34 times.

In this paper, we have compared the individual relative effectiveness of the photochemical reaction of PAFD-FI and PCFD-FI dyads, PAFD and PCFD compounds and a free fluorescein dye. Analysis of the photochemical activity of PCFD-FI in aqueous solution showed that its superoxide generation intensity is more than 15 times higher than the total photochemical activity of individual PCFD and fluorescein (Fig. 6, A and Table 1, line 15). The observed effect confirms the effective transfer of excitation and/or an electron from the fluorescein moiety to the fullerene core. In contrast, the photochemical activity of the PAFD-FI exceeds the total photochemical activity of the PAFD and fluorescein by a factor of 1.24 (Fig. 6, B and Table 1, line 15), indicating a weak interaction of the fullerene core with the dye in this dyad.

The photochemical activity of the investigated dyads agrees well with the experimental absorption and fluorescence spectra and also with the calculated data for the excitation or electron transport efficiency in their structure.

We previously showed an exceptionally high photochemical activity of non-covalent fullerene–fluorescein complexes based on a similar polycationic fullerene derivative [28]. Nevertheless, such non-covalent complexes are easily destroyed by interaction with biological model membranes and could lose their high photochemical activity, as was shown [28]. The presence of a strong covalent bond between fluorescein and the fullerene core allows expecting a high photodynamic activity of the dyads under study in biological media.

4. Conclusion

In summary, we can conclude that electrostatic charges have a significant effect on the conformation of the studied fullerene–dye dyads in an aqueous solution and on their photophysical properties and photochemical activity. The PCFD-FI dyad was shown to take a folded conformation in solution in which the dianion of fluorescein interacts with the cationic addends of the fullerene derivative and partially compensates their charge, decreasing the solubility of this dyad in water.

The proximity of fluorescein to addends of the fullerene derivative and hence to the fullerene core greatly facilitates the transfer of

excitation and/or an electron from the dye to the fullerene. The proximity determines a strong fluorescence quenching in this dyad, and its pronounced photochemical activity.

In contrast, the PAFD-FI dyad has similar negative electrostatic charges on fluorescein and the fullerene derivative, which are spaced as far apart as possible as a result of the electrostatic repulsion. The PAFD-FI dyad consequently has an unfolded conformation with a large distance between dye and fullerene core, which significantly obstructs the excitation and/or electron transfer. Therefore, the PAFD-FI dyad exhibits a much weaker fluorescence quenching and photochemical activity than the PCFD-FI dyad, as shown here. The presence of oppositely charged groups on the fullerene derivative and the dye thus significantly affects the efficiency of deactivation processes not only in non-covalent fullerene–dye complexes but also in covalently linked fullerene–dye dyads.

The electrostatic charges on the dye and addends of fullerene derivative could affect not only the conformation of the dyad but also the solubility of these compounds in water and their ability to interact with cell membranes. This should be taken into account in designing water-soluble fullerene–dye photosensitizers for biomedical applications.

As demonstrated for the fullerene–fluorescein dyad, such fullerene-based structures allow converting the energy of the singlet-excited dye to an effective generation of ROS. This effect significantly broadens the variety of photoactive dyes because nearly every dye with high absorbance in the desirable spectral region could potentially be used to create a highly effective photosensitizer by attaching it to fullerene core.

Conflicts of interest

There are no conflicts to declare.

Acknowledgements

The chemical design and characterization of new water-soluble fullerene derivatives and corresponding dyads were supported by the Russian Foundation for Basic Research (RFBR project No. 16-53-52030). The studies of the photophysical properties and the photochemical activity of dyads were funded by the RFBR research project №

17-34-01156 mol_a and by the FP7-PEOPLE-2013-IRSES project “Multicoloured ambipolar conducting polymers for single polymer optoelectronic devices” (AmbiPOD, Grant agreement no.: PIRSES-GA-2013-612670).

References

- Abrahamse H, Hamblin MR. New photosensitizers for photodynamic therapy. *Biochem J* 2016;473:347–64. <https://doi.org/10.1042/BJ20150942>.
- Yano S, Hirohara S, Obata M, Hagiya Y, Ogura S, Ikeda A, et al. Current states and future views in photodynamic therapy. *J Photochem Photobiol C Photochem Rev* 2011;12:46–67. <https://doi.org/10.1016/j.jphotochemrev.2011.06.001>.
- Plaetzer K, Krammer B, Berlanda J, Berr F, Kiesslich T. Photophysics and photochemistry of photodynamic therapy: fundamental aspects. *Laser Med Sci* 2009;24:259–68. <https://doi.org/10.1007/s10103-008-0539-1>.
- Zhang J, Jiang C, Figueiró Longo JP, Azevedo RB, Zhang H, Muehlmann LA. An updated overview on the development of new photosensitizers for anticancer photodynamic therapy. *Acta Pharm Sin B* 2017;8:137–46. <https://doi.org/10.1016/j.apsb.2017.09.003>.
- Ji S, Ge J, Escudero D, Wang Z, Zhao J, Jacquemin D. Molecular structure–intersystem crossing relationship of heavy-atom-free BODIPY triplet photosensitizers. *J Org Chem* 2015;80:5958–63. <https://doi.org/10.1021/acs.joc.5b00691>.
- Guo S, Sun J, Ma L, You W, Yang P, Zhao J. Visible light-harvesting naphthalene-diimide (NDI)-C60 dyads as heavy-atom-free organic triplet photosensitizers for triplet–triplet annihilation based upconversion. *Dyes Pigments* 2013;96:449–58. <https://doi.org/10.1016/j.dyepig.2012.09.008>.
- Wang M, Huang Y, Sperandio FF, Huang L, Sharma SK, Mroz P, et al. Photodynamic therapy with water-soluble cationic fullerene derivatives. *Springer Ser. Biomater. Sci. Eng* 2016. p. 145–200. https://doi.org/10.1007/978-3-319-22861-7_5.
- Sharma SK, Chiang LY, Hamblin MR. Photodynamic therapy with fullerenes in vivo: reality or a dream? *Nanomedicine* 2011;6:1813–25. <https://doi.org/10.2217/nnm.11.144>.
- Kotelnikova RA, Kotelnikov AI, Bogdanov GN, Romanova VS, Kuleshova EF, Parnes ZN, et al. Membranotropic properties of the water soluble amino acid and peptide derivatives of fullerene C60. *FEBS Lett* 1996;389:111–4. [https://doi.org/10.1016/0014-5793\(96\)00537-6](https://doi.org/10.1016/0014-5793(96)00537-6).
- Friedman SH, DeCamp DL, Sijbesma RP, Srdanov G, Wudl F, Kenyon GL. Inhibition of the HIV-1 protease by fullerene derivatives: model building studies and experimental verification. *J Am Chem Soc* 1993;115:6506–9. <https://doi.org/10.1021/ja00068a005>.
- Fedorova NE, Klimova RR, Tulenev YA, Chichev EV, Kornev AB, Troshin PA, et al. Carboxylic fullerene C60 derivatives: efficient microbicides against herpes simplex virus and cytomegalovirus infections in vitro. *Mendelev Commun* 2012;2:254–6. <https://doi.org/10.1016/j.mencom.2012.09.009>.
- Tat'yanenko LV, Kotel'nikova RA, Poletaeva DA, Dobrokhotova OV, Pikhteleva IY, Kornev AB, et al. Effects of water-soluble polysubstituted fullerene derivatives on sarcoplasmic reticulum Ca²⁺-ATPase and cyclic guanosine monophosphate phosphodiesterase activities. *Pharm Chem J* 2013;47:405–8. <https://doi.org/10.1007/s11094-013-0969-3>.
- Koeppe R, Sariciftci NS. Photoinduced charge and energy transfer involving fullerene derivatives. *Photochem Photobiol Sci* 2006;5:1122–31. <https://doi.org/10.1039/b612933c>.
- Kotel'nikov AI, Rybkin AY, Goryachev NS, Belik AY, Kornev AB, Troshin PA. Photodynamic activity of a hybrid nanostructure based on a polycationic fullerene derivative and phthalocyanine dye photosens. *Dokl Phys Chem* 2013;452:229–32. <https://doi.org/10.1134/S0012501613080046>.
- Kamat JP, Devasagayam TP, Priyadarsini KI, Mohan H. Reactive oxygen species mediated membrane damage induced by fullerene derivatives and its possible biological implications. *Toxicology* 2000;155:55–61.
- Franskevych D, Palyvoda K, Petukhov D, Prylutska S, Grynyuk I, Schuetze C, et al. Fullerene C60 penetration into leukemic cells and its photoinduced cytotoxic effects. *Nanoscale Res Lett* 2017;12:40. <https://doi.org/10.1186/s11671-016-1819-5>.
- Mroz P, Pawlak A, Satti M, Lee H, Wharton T, Gali H, et al. Functionalized fullerenes mediate photodynamic killing of cancer cells: type I versus Type II photochemical mechanism. *Free Radic Biol Med* 2007;43:711–9. <https://doi.org/10.1016/j.freeradbiomed.2007.05.005>.
- Yano S, Naemura M, Toshimitsu A, Akiyama M, Ikeda A, Kikuchi J, et al. Efficient singlet oxygen generation from sugar pendant C60 derivatives for photodynamic therapy. *Chem Commun (J Chem Soc Sect D)* 2015;51:16605–8. <https://doi.org/10.1039/c5cc07353g>.
- Mroz P, Xia Y, Asanuma D, Konopko A, Zhiyentayev T, Huang Y-Y, et al. Intraperitoneal photodynamic therapy mediated by a fullerene in a mouse model of abdominal dissemination of colon adenocarcinoma. *Nanomedicine* 2011;7:965–74. <https://doi.org/10.1016/j.nano.2011.04.007>.
- Shi J, Yu X, Wang L, Liu Y, Gao J, Zhang J, et al. PEGylated fullerene/iron oxide nanocomposites for photodynamic therapy, targeted drug delivery and MR imaging. *Biomaterials* 2013;34:9666–77. <https://doi.org/10.1016/j.biomaterials.2013.08.049>.
- Gsponer NS, Agazzi ML, Spesia MB, Durantini EN. Approaches to unravel pathways of reactive oxygen species in the photoactivation of bacteria induced by a dicationic fulleropyrrolidinium derivative. *Methods* 2016;109:167–74. <https://doi.org/10.1016/j.ymeth.2016.05.019>.
- Spesia MB, Milanesio ME, Durantini EN. Fullerene derivatives in photodynamic inactivation of microorganisms. *Nanostructures Antimicrob. Ther. Nanostructures Ther. Med. Ser.* 2017;1:413–33. <https://doi.org/10.1016/B978-0-323-46152-8.00018-4>.
- Huang L, Xuan Y, Koide Y, Zhiyentayev T, Tanaka M, Hamblin MR. Type I and Type II mechanisms of antimicrobial photodynamic therapy: an in vitro study on gram-negative and gram-positive bacteria. *Laser Surg Med* 2012;44:490–9. <https://doi.org/10.1002/lsm.22045>.
- Käsermann F, Kempf C. Photodynamic inactivation of enveloped viruses by buckminsterfullerene. *Antivir Res* 1997;34:65–70.
- Rud Y, Buchatsky L, Prylutsky Y, Marchenko O, Senenko A, Schütze C, et al. Using C60 fullerenes for photodynamic inactivation of mosquito iridescent viruses. *J Enzym Inhib Med Chem* 2012;27:614–7. <https://doi.org/10.3109/14756366.2011.601303>.
- Kotel'nikov AI, Rybkin AY, Goryachev NS, Belik AY, Troshin PA. Spectral properties and photodynamic activity of complexes of polycationic derivative of fullerene C60 with xanthene dye fluorescein. *Optic Spectrosc* 2016;120:379–85. <https://doi.org/10.1134/S0030400X16030152>.
- Barinov AV, Goryachev NS, Poletaeva DA, Rybkin AY, Kornev AB, Troshin PA, et al. Photodynamic activity of hybrid nanostructure on the basis of polycationic fullerene derivative and xanthene dye eosine Y. *Nanotechnologies Russ* 2012;7:409–14. <https://doi.org/10.1134/S1995078012040039>.
- Belik AY, Rybkin AY, Voronov II, Goryachev NS, Volyniuk D, Grazulevicius JV, et al. Non-covalent complexes of polycationic fullerene C60 derivative with xanthene dyes – spectral and photochemical properties in water and in liposomes. *Dyes Pigments* 2017;139:65–72. <https://doi.org/10.1016/j.dyepig.2016.11.025>.
- Pal D, Ray A, Bhattacharya S. Influence of the energy of charge transfer on non-covalent interactions between fullerenes and a designed bisporphyrin. *Spectrochim Acta Part A Mol Biomol Spectrosc* 2012;95:317–30. <https://doi.org/10.1016/j.saa.2012.03.083>.
- Ray A, Pal H, Bhattacharya S. Photophysical investigations on supramolecular fullerene/phthalocyanine charge transfer interactions in solution. *Spectrochim Acta Mol Biomol Spectrosc* 2014;117:686–95. <https://doi.org/10.1016/j.saa.2013.08.107>.
- Berera R, Moore GF, van Stokkum IHM, Kodis G, Liddell P a, Gervaldo M, et al. Charge separation and energy transfer in a caroteno-C60 dyad: photoinduced electron transfer from the carotenoid excited states. *Photochem Photobiol Sci* 2006;5:1142–9. <https://doi.org/10.1039/b613971j>.
- Remón P, Carvalho P, Baleizo C, Berberan MN, Parente Carvalho C, Baleizão C, et al. Highly efficient singlet-singlet energy transfer in light-harvesting [60,70] fullerene-4-amino-1,8-naphthalimide dyads. *ChemPhysChem* 2013;3:2717–24. <https://doi.org/10.1002/cphc.201300424>.
- Liu Y, Zhao J. Visible light-harvesting perylenebisimide-fullerene (C60) dyads with bidirectional “ping-pong” energy transfer as triplet photosensitizers for photo-oxidation of 1,5-dihydroxynaphthalene. *Chem Commun (J Chem Soc Sect D)* 2012;48:3751–3. <https://doi.org/10.1039/c2cc30345k>.
- Wu W, Zhao J, Sun J, Guo S. Light-harvesting fullerene dyads as organic triplet photosensitizers for triplet-triplet annihilation upconversions. *J Org Chem* 2012;77:5305–12. <https://doi.org/10.1021/jo300613g>.
- Poletaeva DA, Kotel'nikova RA, Mischenko DV, Rybkin AY, Smolina AV, Faingold II, et al. Estimation of membrane activity of water-soluble polysubstituted fullerene derivatives by luminescence methods. *Nanotechnologies Russ* 2012;7:302–7. <https://doi.org/10.1134/S1995078012030135>.
- Kotelnikov AI, Rybkin AY, Khakina EA, Kornev AB, Barinov AV, Goryachev NS, et al. Hybrid photoactive fullerene derivative-ruboxyl nanostructures for photodynamic therapy. *Org Biomol Chem* 2013;11:4397–404. <https://doi.org/10.1039/c3ob40136g>.
- Lu F, Haque SA, Yang S-T, Luo PG, Gu L, Kitaygorodskiy A, et al. Aqueous compatible fullerene-doxorubicin conjugates. *J Phys Chem C Nanomater Interfaces* 2009;113:17768. <https://doi.org/10.1021/jp906750z>.
- Chaudhuri P, Paraskar A, Soni S, Mashelkar R a, Sengupta S. Fullerene-cytotoxic conjugates for cancer chemotherapy. *ACS Nano* 2009;3:2505–14. <https://doi.org/10.1021/nn900318y>.
- Wang F, Cui X, Lou Z, Zhao J, Bao M, Li X. Switching of the triplet excited state of rhodamine-C60 dyads. *Chem Commun (J Chem Soc Sect D)* 2014;50:2–5. <https://doi.org/10.1039/c4cc07603f>.
- Yin R, Wang M, Huang Y-Y, Huang H-C, Avci P, Chiang LY, et al. Photodynamic therapy with decacationic [60]fullerene monoadducts: effect of a light absorbing electron-donor antenna and micellar formulation. *Nanomedicine* 2014;10:795–808. <https://doi.org/10.1016/j.nano.2013.11.014>.
- Guan M, Ge J, Wu J, Zhang G, Chen D, Zhang W, et al. Fullerene/photosensitizer nanovesicles as highly efficient and clearable phototheranostics with enhanced tumor accumulation for cancer therapy. *Biomaterials* 2016;103:75–85. <https://doi.org/10.1016/j.biomaterials.2016.06.023>.
- Khakina EA, Yurkova AA, Peregodov AS, Troyanov SI, Trush VV, Vovk AI, et al. Highly selective reactions of C60Cl6 with thiols for the synthesis of functionalized [60]fullerene derivatives. *Chem Commun (J Chem Soc Sect D)* 2012;48:7158–60. <https://doi.org/10.1039/c2cc32517a>.
- Troshina OA, Troshin PA, Peregodov AS, Kozlovskiy VI, Balzarini J, Lyubovskaya RN. Chlorofullerene C60Cl6: a precursor for straightforward preparation of highly water-soluble polycarboxylic fullerene derivatives active against HIV. *Org Biomol Chem* 2007;5:2783. <https://doi.org/10.1039/b705331b>.
- Stewart JJP. Computational chemistry MOPAC2016 Version: 16353W 2016 <http://openmopac.net>.
- Stewart JJP. Optimization of parameters for semiempirical methods VI: more modifications to the NDDO approximations and re-optimization of parameters. *J Mol Model* 2013;19:1–32. <https://doi.org/10.1007/s00894-012-1667-x>.

- [46] Yamakoshi Y, Umezawa N, Ryu A, Arakane K, Miyata N, Goda Y, et al. Active oxygen species generated from photoexcited fullerene (C60) as potential medicines: O₂^{-•} versus 1O₂. *J Am Chem Soc* 2003;125:12803–9. <https://doi.org/10.1021/ja0355574>.
- [47] Hashimoto A, Yamanaka T, Takamura-Enya T. Synthesis of novel fluorescently labeled water-soluble fullerenes and their application to its cellular uptake and distribution properties. *J Nanoparticle Res* 2017;19. <https://doi.org/10.1007/s11051-017-4098-x>.
- [48] Xu K, Liu F, Ma J, Tang B. A new specific fullerene-based fluorescent probe for trypsin. *Analyst (Cambridge, UK)* 2011;136:1199. <https://doi.org/10.1039/c0an00576b>.
- [49] Lucafò M, Pacor S, Fabbro C, Da Ros T, Zorzet S, Prato M, et al. Study of a potential drug delivery system based on carbon nanoparticles: effects of fullerene derivatives in MCF7 mammary carcinoma cells. *J Nanoparticle Res* 2012;14:1–13. <https://doi.org/10.1007/s11051-012-0830-8>.
- [50] Huang L, Terakawa M, Zhiyentayev T, Huang Y-Y, Sawayama Y, Jahnke A, et al. Innovative cationic fullerenes as broad-spectrum light-activated antimicrobials. *Nanomedicine* 2010;6:442–52. <https://doi.org/10.1016/j.nano.2009.10.005>.
- [51] Patel MB, Harikrishnan U, Valand NN, Mehta DS, Joshi KV, Kumar SP, et al. Novel cationic fullerene derivatized s-triazine scaffolds as photoinduced DNA cleavage agents: design, synthesis, biological evaluation and computational investigation. *RSC Adv* 2013;3:8734. <https://doi.org/10.1039/c3ra40950c>.
- [52] Kotelnikova RA, Smolina AV, Grigoryev VV, Faingold II, Mischenko DV, Rybkin AY, et al. Influence of water-soluble derivatives of [60]fullerene on therapeutically important targets related to neurodegenerative diseases. *Med Chem Commun* 2014;5:1664–8. <https://doi.org/10.1039/C4MD00194J>.
- [53] Kornev AB, Peregudov AS, Martynenko VM, Guseva GV, Sashenkova TE, Rybkin AY, et al. Synthesis and biological activity of a novel water-soluble methano[60] fullerene tetracarboxylic derivative. *Mendeleev Commun* 2013;23:323–5. <https://doi.org/10.1016/j.mencom.2013.11.006>.
- [54] Hua J, Meng F, Ding F, Li F, Tian H. Novel soluble and thermally-stable fullerene dyad containing perylene. *J Mater Chem* 2004;14:1849. <https://doi.org/10.1039/b316996k>.
- [55] Ray A, Chattopadhyay S, Bhattacharya S. Photophysical and theoretical insights on non-covalently linked fullerene–zinc phthalocyanine complexes. *Spectrochim Acta Part A Mol Biomol Spectrosc* 2011;79:1435–42. <https://doi.org/10.1016/j.saa.2011.04.083>.
- [56] Förster T. Zwischenmolekulare Energiewanderung und Fluoreszenz. *Ann Phys* 1948;437:55–75. <https://doi.org/10.1002/andp.19484370105>.
- [57] Kotelnikov AI. The analysis of experimental data on electron conductivity of globular proteins. *Biofizika* 1993;38:228–32.
- [58] Moser CC, Keske JM, Warncke K, Farid RS, Dutton PL. Nature of biological electron transfer. *Nature* 1992;355:796–802. <https://doi.org/10.1038/355796a0>.
- [59] Gray HB, Winkler JR. Heme protein dynamics: electron tunneling and redox triggered folding. In: Kadish KM, Smith KM, Guillard R, editors. *Porphyr. Handbook, Bioinorg. Bioorganic chem Amsterdam*: Elsevier; 2003. p. 51–73. <https://doi.org/10.1016/B978-0-08-092385-7.50008-2>.
- [60] Levich VG, Dogonadze RR. Theory of non-radiation electron transitions from ion to ion in solutions. *Dokl Akad Nauk SSSR* 1959;124:123–6.
- [61] Marcus RA, Sutin N. Electron transfers in chemistry and biology. *Biochim Biophys Acta* 1985;811:265–322. [https://doi.org/10.1016/0304-4173\(85\)90014-X](https://doi.org/10.1016/0304-4173(85)90014-X).
- [62] Guo S, Xu L, Xu K, Zhao J, Küçüköz B, Karatay A, et al. Bodipy–C60 triple hydrogen bonding assemblies as heavy atom-free triplet photosensitizers: preparation and study of the singlet/triplet energy transfer. *Chem Sci* 2015;6:3724–37. <https://doi.org/10.1039/C4SC03865G>.
- [63] Zhou S, Burger C, Chu B, Sawamura M, Nagahama N, Toganoh M, et al. Spherical bilayer vesicles of fullerene-based surfactants in water: a laser light scattering study. *Science* 2001;291:1944–7. <https://doi.org/10.1126/science.291.5510.1944>.
- [64] Kato H, Kaneta N, Nii S, Kobayashi K, Fukui N, Shinohara H, et al. Preparation and supramolecular properties of unadulterated glycosyl liposomes from a bis(α-D-mannopyranosyl)-[60]fullerene conjugate. *Chem Biodivers* 2005;2:1232–41. <https://doi.org/10.1002/cbdv.200590093>.
- [65] Chernyak AV, Avilova IA, Khakina EA, Mumyatov AV, Zabrodin VA, Troshin PA, et al. Supramolecular self-organization of fullerene derivatives in solutions studied by pulsed field gradient NMR technique. *Appl Magn Reson* 2016;47:859–68. <https://doi.org/10.1007/s00723-016-0784-6>.
- [66] Lettinga MP, Zuilhof H, van Zandvoort MAMJ. Phosphorescence and fluorescence characterization of fluorescein derivatives immobilized in various polymer matrices. *Phys Chem Chem Phys* 2000;2:3697–707. <https://doi.org/10.1039/a909707d>.